at 3/2013

Fast and Saturating Thrust Direction Control for a Quadrotor Helicopter

Schnelle und sättigende Regelung der Schubrichtung eines Quadrocopters

Oliver Fritsch*, Bernd Henze, Boris Lohmann, Technische Universität München

* Correspondence author: oliver.fritsch@tum.de

Summary In this paper we design a continuous, nonlinear state feedback controller that aligns the body-fixed thrust direction of a quadrotor helicopter with a constant desired direction given in an inertial coordinate system. The controller is designed based on an energy shaping approach and is able to saturate the control torques. Almost global asymptotic stability of the desired thrust direction is proven for arbitrary unknown moment of inertia matrices. Performance of the closed loop system is verified by simulations. ►►► **Zusammenfassung** In diesem Beitrag wird ein kontinuierlicher nichtlinearer Zustandsregler entworfen, der die körperfeste Schubrichtung eines Quadrocopters mit einer gewünschten inertialen Richtung in Übereinstimmung bringt. Der Regler wird über einen energiebasierten Ansatz entworfen und ist in der Lage die Stellmomente zu sättigen. Für beliebige unbekannte Massenträgheitsmomente wird gezeigt, dass die Wunschrichtung asymptotisch stabil ist und der Einzugsbereich, abgesehen von einem Unterraum mit Maß Null, den gesamten Zustandsraum umfasst. Die Leistungsfähigkeit der Regelung wird in Simulationen verifiziert.

Keywords Reduced attitude control, quadrotor UAV, saturating control, energy shaping, quaternions ►►►
Schlagwörter Reduzierte Fluglagenregelung, Quadrocopter, sättigende Regelung, energiebasierte Regelung, Quaternionen

1 Introduction

A quadrotor helicopter is a very agile vertical take-off and landing aircraft, which offers the ability of hovering. As shown in Fig. 1 it consists of a cross-shaped rigid frame with one rotor at each end. Usually the rotor dynamics are very fast. Hence, the angular velocities of the single rotors or the equivalent thrusts $f_1 \ldots f_4$ can be regarded as the control inputs of the nonlinear system. It is well known (see e. g. [21]) that these four thrusts can be converted into a total thrust u perpendicular to the frame and a torque vector $\boldsymbol{\tau} = [\tau_x \;\; \tau_y \;\; \tau_z]^T$ acting on the center of mass of the vehicle. Consequently, u and $\boldsymbol{\tau}$ are an alternative choice of control inputs used in the following. Since the direction of the (total) thrust is body-fixed, the execution of almost all translational motions requires tilting the whole quadrotor helicopter. Consequently, a fast and robust thrust direction control can be regarded as the basis for the control of any translational motion. The desired thrust direction may be the output of a higher level position controller or simply the remote control command of a human operator. Note that controlling the thrust direction does not require to control the orientation of the quadrotor helicopter around its thrust axis. Thus, compared to a complete attitude control one rotational degree of freedom can be left unspecified. Based on an energy shaping approach, we present a continuous state feedback controller taking advantage of this additional degree of freedom by forcing the thrust axis towards the desired direction as direct as possible. At the same time the full nonlinear nature of the problem and control input constraints are considered. Moreover, the controller is able to exploit the available control torques to a great extent or even saturate them during the regulation process guaranteeing a very fast transient behavior. The controller asymptotically stabilizes the desired thrust direction for all initial states except for a set of zero meas-

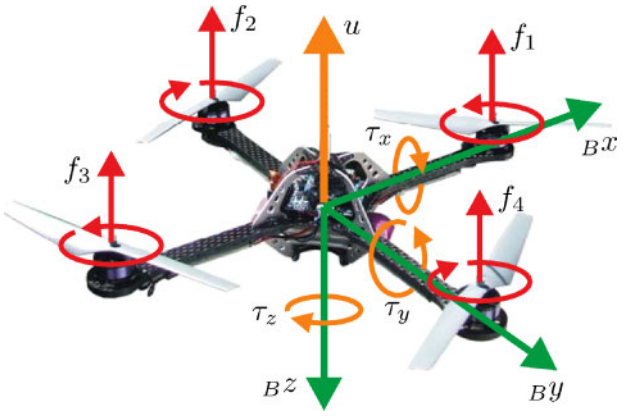

Figure 1 Quadrotor helicopter with body-fixed coordinate system B and alternative control inputs $f_1 \ldots f_4$ or $u, \tau_x, \tau_y, \tau_z$.

ure. We will refer to this type of stability as almost global asymptotic stability and we will show that this property holds for arbitrary uncertainties in the moment of inertia matrix. Since it is well known that in any kind of attitude control problem no continuous control law can achieve global asymptotic stability [2], almost global asymptotic stability is the best we can achieve with a continuous control law.

In most of the literature on quadrotor helicopters only complete attitude control is addressed. Since the quadrotor helicopter is usually treated as a rigid body, the problem is equivalent to the broad field of attitude control for rigid bodies. Various control strategies like PD control [10; 22], sliding mode control [3], geometric control [15], inverse optimal control [13], H_∞-control [6], hybrid control [16] and many others [18; 20; 21] can be found. Only a few works consider control input constraints [1; 8; 12] and even less address thrust direction control or analogous problems [5; 9].

In Sect. 2 we give a brief introduction into attitude parametrization using quaternions and the required mathematical background. A detailed problem statement is presented in Sect. 3, before the plant dynamics and control input constraints are introduced in Sect. 4. Based on an energy shaping approach the thrust direction controller is developed in Sect. 5 and almost global asymptotic stability of the set of admissible equilibrium points is proven. In Sect. 6 the performance of the controller is studied in simulations before conclusions are drawn in Sect. 7 along with an outlook for future research.

2 Attitude Parametrization

Two coordinate systems are necessary to specify the attitude of an aircraft: a body-fixed coordinate system B attached to the aircraft and an inertial reference coordinate system, which moves along with the aircraft but is nonrotating. Within this paper, a *North East Down* coordinate system N serves as reference system. The origins of both coordinate systems are located at the center of mass of the vehicle. As shown in Fig. 1 the xy-plane of the body-fixed system B lies in the plane of the cross-shaped frame of the quadrotor helicopter and the z-axis points to the bottom side of the frame. Hence the thrust vector in body coordinates always points in the negative z-direction. It follows that aligning the thrust direction of the quadrotor helicopter with a desired direction is equivalent to aligning the z-axis of the body-fixed frame with the corresponding negative direction.

One way of parameterizing the relation between two coordinate systems is the use of quaternions (see e. g. [19; 23]) which are directly built up by the axis and the angle information of a rotation. This parametrization admits an advantageous decomposition into two principal rotations which is a crucial step for the development of our control law. In a different context this decomposition has already been presented in [4] and [7].

Interpretation of a Quaternion

A quaternion $\mathbf{q} \in \mathcal{S}^3$ with $\mathcal{S}^3 = \{\mathbf{q} \in \mathbb{R}^4 \mid \mathbf{q}^T\mathbf{q} = 1\}$ can be used to describe the rotation that maps a coordinate system X on a coordinate system Y. The four elements of a quaternion $\mathbf{q}$ are composed of the angle and axis information of the corresponding rotation. It holds that

$$\mathbf{q} = \begin{bmatrix} q_1 \\ q_2 \\ q_3 \\ q_4 \end{bmatrix} = \begin{bmatrix} \mathbf{a} \sin \dfrac{\alpha}{2} \\ \cos \dfrac{\alpha}{2} \end{bmatrix} \tag{1}$$

where $\mathbf{a} \in \mathbb{R}^3$ is the axis vector and α is the rotation angle. Since $\mathbf{a}$ is chosen to be a unit vector, $\mathbf{q}$ is also of length one and therefore is referred to as a *unit quaternion*. From (1) it is clear that $-\mathbf{q}$ describes a rotation with angle $\alpha \pm (2k+1)\cdot 2\pi$, $k \in \mathbb{N}_0$ about the same axis $\mathbf{a}$ and therefore also represents the mapping from X to Y. According to (1) the reverse rotation from Y to X is given by the conjugate quaternion

$$\bar{\mathbf{q}} = \begin{bmatrix} -q_1 & -q_2 & -q_3 & q_4 \end{bmatrix}^T . \tag{2}$$

Multiplication of Quaternions

The multiplication of two quaternions is defined as

$$\mathbf{r} = \mathbf{q} \circ \mathbf{p} = \underbrace{\begin{bmatrix} p_4 & p_3 & -p_2 & p_1 \\ -p_3 & p_4 & p_1 & p_2 \\ p_2 & -p_1 & p_4 & p_3 \\ -p_1 & -p_2 & -p_3 & p_4 \end{bmatrix}}_{\mathbf{W}(\mathbf{p})} \begin{bmatrix} q_1 \\ q_2 \\ q_3 \\ q_4 \end{bmatrix} \tag{3}$$

and corresponds to a consecutive execution of the rotations parametrized by $\mathbf{q}$ and $\mathbf{p}$. The second rotation defined by $\mathbf{p}$ is specified in the coordinate system resulting from the first rotation $\mathbf{q}$. Note that $\mathbf{W}$ is an orthonormal matrix.

Kinematics

If $\mathbf{q}$ describes the rotation from a coordinate system X to a coordinate system Y and $\boldsymbol{\omega} = [\omega_x \;\; \omega_y \;\; \omega_z]^T$ denotes the

angular velocity of X with respect to Y given in X, then the derivative $\dot{\mathbf{q}}$ is given by

$$\dot{\mathbf{q}} = -\frac{1}{2}\mathbf{W}(\mathbf{q})\begin{bmatrix}\boldsymbol{\omega}\\0\end{bmatrix} = -\frac{1}{2}\mathbf{W}_R(\mathbf{q})\boldsymbol{\omega} \tag{4}$$

where $\mathbf{W}_R(\mathbf{q})$ is equal to $\mathbf{W}(\mathbf{q})$ without the last column.

Decomposition into Principal Rotations
With the modified sign function

$$\overline{\operatorname{sgn}}(a) = \begin{cases} 1 & \text{if} \quad a \geq 0 \\ -1 & \text{if} \quad a < 0 \end{cases} \tag{5}$$

and a given quaternion $\mathbf{q}$ mapping X on Y it is clear from the preceding discussion that $\hat{\mathbf{q}} = \overline{\operatorname{sgn}}(q_4)\cdot\mathbf{q}$ represents the same mapping but with $\hat{\alpha} = 2\cdot\arccos(\hat{q}_4) \in [0,\pi]$ being the smallest possible rotation angle. With that in mind, we decompose $\mathbf{q}$ into a product of two quaternions $\mathbf{q}_{xy}$ and $\mathbf{q}_z$ yielding

$$\mathbf{q} = \hat{\mathbf{q}}\cdot\overline{\operatorname{sgn}}(q_4) = (\mathbf{q}_{xy}\circ\mathbf{q}_z)\cdot\overline{\operatorname{sgn}}(q_4)\,. \tag{6}$$

Herein the quaternion $\mathbf{q}_{xy}$ describes how the z-axis of Y is tilted against the z-axis of X. The resulting coordinate system is referred to as the *auxiliary system* A, see Fig. 2. The rotation from the system X to the auxiliary system A is around an axis $\mathbf{a}_{xy}$ in the xy-plane, which causes $\mathbf{q}_{xy}$ to be of the structure

$$\mathbf{q}_{xy} = \begin{bmatrix} q_x & q_y & 0 & q_p \end{bmatrix}^T\,. \tag{7}$$

The second quaternion $\mathbf{q}_z$ describes the remaining rotation around the z-axis of the frame A and thus has the structure

$$\mathbf{q}_z = \begin{bmatrix} 0 & 0 & q_z & q_w \end{bmatrix}^T\,. \tag{8}$$

Using (7) and (8) and applying rule (3) the product (6) can be written as

$$\mathbf{q} = \begin{bmatrix} q_w q_x + q_z q_y & q_w q_y - q_z q_x & q_z q_p & q_w q_p \end{bmatrix}^T \cdot \overline{\operatorname{sgn}}(q_4)\,. \tag{9}$$

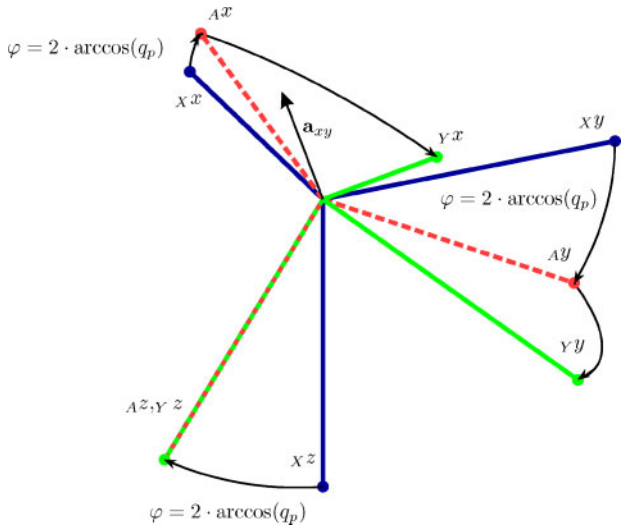

Figure 2 Initial coordinate system X, auxiliary coordinate system A and target coordinate system Y.

Note that because of (6), $q_w q_p \geq 0$. By defining $q_p \geq 0$ we also establish $q_w \geq 0$, which means that $\mathbf{q}_{xy}$ and $\mathbf{q}_z$ always describe the smallest possible rotations. The derivative of $\mathbf{q}_{xy}$ with respect to time is

$$\dot{\mathbf{q}}_{xy} = \begin{bmatrix}\dot{q}_x\\ \dot{q}_y\\ 0\\ \dot{q}_p\end{bmatrix} = \frac{1}{2}\begin{bmatrix} \frac{q_y^2 - q_p^2}{q_p} & -\frac{q_x q_y}{q_p} & 2q_y \\ -\frac{q_x q_y}{q_p} & \frac{q_x^2 - q_p^2}{q_p} & -2q_x \\ 0 & 0 & 0 \\ q_x & q_y & 0 \end{bmatrix}\boldsymbol{\omega} \tag{10}$$

and follows from (7), (8), (6), (3), (4), the exploitation of the unit length of the quaternions and $(\mathbf{q}_{xy})_3 \equiv 0$. Note that $\mathbf{q}_{xy}$ evolves continuously as long as $q_p \neq 0$.

3 Problem Statement

Let the attitude of the quadrotor helicopter be parametrized by the quaternion $\mathbf{q}_b$ which describes the rotation that maps the inertial coordinate system N on the body-fixed system B. Then the objective is to design a control law which aligns the z-axis of B with a desired constant direction. The desired direction is given by the z-axis of a coordinate system D, whose orientation with respect to N is specified by the quaternion $\mathbf{q}_d$. According to (3) and (2)

$$\mathbf{q} = \bar{\mathbf{q}}_b \circ \mathbf{q}_d \tag{11}$$

is the rotation error between the coordinate system B and D. Further decomposition of the error quaternion

$$\mathbf{q} = (\mathbf{q}_{xy}\circ\mathbf{q}_z)\cdot\overline{\operatorname{sgn}}(q_4) \tag{12}$$

into the two rotations $\mathbf{q}_{xy}$ and $\mathbf{q}_z$, as in (6), shows that the error between the z-axis of B and the z-axis of D is completely described by the first rotation $\mathbf{q}_{xy}$. With $\boldsymbol{\omega}$ being the angular velocity of the quadrotor helicopter given in B the control objective can thus be formulated as

$$\mathbf{q}_{xy} \to \begin{bmatrix} 0 & 0 & 0 & 1 \end{bmatrix}^T, \quad \boldsymbol{\omega} \to \mathbf{0} \quad \text{as} \quad t \to \infty\,. \tag{13}$$

With (9) the equivalence

$$\begin{aligned}\mathbf{q}_{xy} = \begin{bmatrix} 0 & 0 & 0 & 1 \end{bmatrix}^T \Leftrightarrow \mathbf{q} &= \begin{bmatrix} 0 & 0 & q_3 & q_4 \end{bmatrix}^T \\ &= \mathbf{q}_z\cdot\overline{\operatorname{sgn}}(q_4)\end{aligned} \tag{14}$$

can be identified and thus (13) describes a compact set of desired equilibrium points.

4 Plant Model

Regarding the quadrotor helicopter as a rigid body and neglecting the weak gyroscopic effects of the rotors the attitude error dynamics are given by

$$\dot{\mathbf{q}} = -\frac{1}{2}\mathbf{W}_R(\mathbf{q})\boldsymbol{\omega} \tag{15}$$

$$\dot{\boldsymbol{\omega}} = \mathbf{J}^{-1}(\mathbf{J}\boldsymbol{\omega}\times\boldsymbol{\omega}) + \mathbf{J}^{-1}\boldsymbol{\tau} \tag{16}$$

where the state $\mathbf{x} = [\mathbf{q}\ \ \boldsymbol{\omega}]^T \in \mathcal{X}$ with $\mathcal{X} = \mathcal{S}^3 \times \mathbb{R}^3$ is defined as in the previous section, $\mathbf{J} = \mathbf{J}^T > \mathbf{0}$ is the moment of inertia matrix given in B, and $\boldsymbol{\tau}$ is the control torque produced by the rotors given in B. For a quadrotor helicopter the available control torque in the xy-plane is significantly larger than the available control torque in the z-direction. This is due to the fact that the rotors mainly produce forces in the negative body-fixed z-direction which, multiplied with their lever arms, give the control torque in the xy-plane. In contrast, the rotors produce only little aerodynamic drag torques around their rotation-axis which, summed up, give the z-component of the control torque. With that in mind, we assume that the components of the control torque $\boldsymbol{\tau} = [\tau_x\ \ \tau_y\ \ \tau_z]^T$ are bounded as follows:

$$\sqrt{\tau_x^2 + \tau_y^2} \le \bar{\tau}_{xy}\,, \quad |\tau_z| \le \bar{\tau}_z\,, \tag{17}$$

where $\bar{\tau}_{xy}$ and $\bar{\tau}_z$ are positive constants and $\bar{\tau}_{xy} \gg \bar{\tau}_z$.

5 Controller Design

5.1 Basic Idea

The control law is based on an energy shaping approach (see e. g. [17]). This means to select a control action such that the closed-loop dynamics is described by means of a new total energy function with a minimum at the desired operating point. For the problem of thrust direction control only the potential energy E_{pot} is shaped while the kinetic energy part remains the rotational energy E_{rot} of the quadrotor helicopter. Since the system is fully actuated regarding the attitude, we can assign any potential energy function, only restricted by the boundedness of the control inputs. Then, the total energy function of the closed loop system is expressed as

$$V(\mathbf{x}) = E_{rot}(\boldsymbol{\omega}) + E_{pot}(\mathbf{q}) = \frac{1}{2}\boldsymbol{\omega}^T\mathbf{J}\boldsymbol{\omega} + E_{pot}(\mathbf{q}) \tag{18}$$

with V having a strict minimum at the set of operation points defined by (13). Taking the derivative of V and inserting (15) and (16) we get

$$\begin{aligned}\dot{V}(\mathbf{x}) &= \boldsymbol{\omega}^T\mathbf{J}\dot{\boldsymbol{\omega}} + \frac{\partial E_{pot}(\mathbf{q})}{\partial \mathbf{q}}\dot{\mathbf{q}} \\ &= \boldsymbol{\omega}^T\boldsymbol{\tau} - \underbrace{\frac{1}{2}\frac{\partial E_{pot}(\mathbf{q})}{\partial \mathbf{q}}\mathbf{W}_R(\mathbf{q})}_{\mathbf{T}^T(\mathbf{q})}\boldsymbol{\omega}\end{aligned} \tag{19}$$

wherein $\mathbf{T}(\mathbf{q})$ can be identified as the torque field resulting from the potential energy. Now choosing

$$\boldsymbol{\tau} = \mathbf{T}(\mathbf{q}) - \mathbf{D}(\mathbf{x})\boldsymbol{\omega}\,, \tag{20}$$

with $\mathbf{D}(\mathbf{x}) \ge \mathbf{0}$ a positive semidefinite damping matrix, the derivative $\dot{V}$ becomes

$$\dot{V} = -\boldsymbol{\omega}^T\mathbf{D}(\mathbf{x})\boldsymbol{\omega} \le 0\,. \tag{21}$$

This already guarantees stability of the desired thrust direction. To prove asymptotic stability La Salle's invariance principle can be applied.

5.2 Design of the Potential Energy

The assigned potential energy is inspired by the potential energy of a rod-shaped pendulum mounted on a ball joint and exposed to the gravity field of earth. Regarding the pendulum as the current thrust direction and assuming the desired thrust direction points downwards such a pendulum shows the desired features of a thrust direction control: Provided appropriate damping is active in the system, the pendulum swings down and comes to rest in the desired position from almost any initial state. Note that the orientation of the pendulum around its own axis can be arbitrary. On the other hand, the pendulum example exhibits also undesirable features especially regarding the exploitation of the "control torque": The gravity induced torque is proportional to the sine of the deflection angle and thus the maximum torque only appears once for an error angle of $\pi/2$.

In the following we design a potential energy function with the following features:

- Analogous to a torsion spring, the torque induced by the potential energy grows linearly with the error angle φ near the desired thrust direction.
- If the error angle φ exceeds a lower threshold $\varphi_l \ll \pi$, the induced torque stays constant to account for the bounded controls.
- If the error angle φ exceeds an upper threshold φ_u near π, the induced torque decreases linearly and diminishes if the error angle is π rendering the torque continuous over the whole attitude space.

According to the decomposition (6) the positive error angle between the current and the desired thrust direction is given as

$$\varphi = 2 \cdot \arccos(q_p)\,. \tag{22}$$

With a lower and an upper threshold $0 < \varphi_l < \varphi_u < \pi$ and a stiffness coefficient $\bar{\tau}_{xy}/\varphi_l > c_\varphi > 0$ we define

$$T_\varphi(\varphi) = \begin{cases} c_\varphi \cdot \varphi & \text{if} \quad 0 \le \varphi \le \varphi_l \\ c_\varphi \cdot \varphi_l & \text{if} \quad \varphi_l < \varphi \le \varphi_u \\ c_\varphi \varphi_l \cdot \dfrac{\pi - \varphi}{\pi - \varphi_u} & \text{if} \quad \varphi_u < \varphi \le \pi \end{cases} \tag{23}$$

as the magnitude of the torque induced by the potential energy, which acts in the direction of decreasing φ. In terms of φ we can thus construct E_{pot} by integration

$$\begin{aligned} E_{pot}(\varphi) &= \int_0^\varphi T_\varphi(\varphi)\, d\varphi = \\ &= \begin{cases} E_l(\varphi) = \frac{1}{2}c_\varphi\varphi^2 & \text{if} \quad 0 \le \varphi \le \varphi_l \\ E_m(\varphi) = E_l(\varphi_l) + c_\varphi\varphi_l(\varphi - \varphi_l) & \text{if} \quad \varphi_l < \varphi \le \varphi_u \\ E_u(\varphi) & \text{if} \quad \varphi_u < \varphi \le \pi \end{cases} \end{aligned} \tag{24}$$

where

$$E_u(\varphi) = E_m(\varphi_u) + \frac{c_\varphi\varphi_l}{\pi - \varphi_u} \cdot \left(\pi(\varphi - \varphi_u) - \frac{1}{2}(\varphi^2 - \varphi_u^2)\right)\,. \tag{25}$$

According to (19) we can identify the induced torque vector $\mathbf{T}$ by taking the time derivative of E_{pot}. Using (22) and (10) and substituting with (23) one obtains

$$\begin{aligned}\dot{E}_{pot}(\mathbf{x}) &= \frac{\partial E_{pot}(\mathbf{q})}{\partial \mathbf{q}}\dot{\mathbf{q}} = \frac{dE_{pot}(\varphi)}{d\varphi}\cdot\frac{d\varphi(q_p)}{dq_p}\cdot\dot{q}_p \\ &= T_\varphi(\varphi)\cdot\Bigg(\overbrace{\underbrace{-\frac{1}{\sqrt{1-q_p^2}}\begin{bmatrix}q_x & q_y & 0\end{bmatrix}}_{\mathbf{a}_{xy}^T}\boldsymbol{\omega}}^{\dot{\varphi}}\Bigg) \\ &= -\mathbf{T}(\mathbf{q})^T\boldsymbol{\omega} = -\begin{bmatrix}T_x & T_y & 0\end{bmatrix}\boldsymbol{\omega}\,. \end{aligned} \tag{26}$$

Note that the vector $\mathbf{a}_{xy}$ is the unit vector describing the rotation axis of $\mathbf{q}_{xy}$. Note also that E_{pot} can only change when the projection of $\boldsymbol{\omega}$ onto $\mathbf{a}_{xy}$ is nonzero. The potential energy decreases if $\mathbf{a}_{xy}^T\boldsymbol{\omega}$ is positive and it grows if $\mathbf{a}_{xy}^T\boldsymbol{\omega}$ is negative. The subspace of $\mathbb{R}^3$ which does not contribute to a change of E_{pot} is spanned by the two unit vectors

$$\mathbf{a}_\perp = \frac{1}{\sqrt{1-q_p^2}}\begin{bmatrix}q_y & -q_x & 0\end{bmatrix}^T, \quad \mathbf{a}_z = \begin{bmatrix}0 & 0 & 1\end{bmatrix}^T. \tag{27}$$

Together with $\mathbf{a}_{xy}$ they form an orthogonal basis of $\mathbb{R}^3$.

Remark 1. The decomposition (6) is discontinuous and not unique if $\mathbf{q} = [q_1\ \ q_2\ \ 0\ \ 0]^T \Leftrightarrow q_p = 0$. Then, for any quaternion $\mathbf{q}_{xy} = [q_x\ \ q_y\ \ 0\ \ 0]^T$ there can be found a suitable $\mathbf{q}_z$ such that (6) is fulfilled and vice versa. Since according to (22) $\varphi = \pi$ holds, this case corresponds to all orientations where the current thrust direction points in the opposite direction of the desired thrust direction. Note that nevertheless $\mathbf{T}$ is unique and continuous, since $T_\varphi(\pi) = 0$. Similarly if $\mathbf{q}_{xy} = [0\ \ 0\ \ 0\ \ 1]$, meaning that the current thrust direction is perfectly aligned with the desired thrust direction, then the direction of the unit vector $\mathbf{a}_{xy}$ is undefined. Again, $\mathbf{T}$ is unique and continuous, since $T_\varphi(0) = 0$.

5.3 Damping Injection

To complete the control law (20) the damping matrix $\mathbf{D}(\mathbf{x})$ has to be defined. From (21) it is clear that the decrease of V can be amplified by adding positive damping. However, that does not necessarily improve the overall performance of the control system. Especially when aiming at a fast control little damping or even no damping might be advantageous in some situations. Consider for example an initial thrust direction far away from the desired one and an angular velocity with a small component $\mathbf{a}_{xy}^T\boldsymbol{\omega} > 0$ that moves the current thrust direction towards the desired one. Any damping of that component would act against the accelerating torque $\mathbf{T}$ induced by the potential energy and thus would slow down the regulation process. Of course the other components $\mathbf{a}_\perp^T\boldsymbol{\omega}$ and $\mathbf{a}_z^T\boldsymbol{\omega}$ of the angular velocity, that do not contribute to a decrease of φ, should always be damped. In another situation, in which the current thrust direction is close to the desired one and the angular velocity is high, a considerable damping of all components of $\boldsymbol{\omega}$ is desirable. Summing up the preceding thoughts, the damping should not only vary with the state but also distinguish between desirable and undesirable directions of $\boldsymbol{\omega}$.

We incorporate that behavior into the damping by choosing

$$\begin{aligned}\mathbf{D}(\mathbf{x}) &= \kappa_1(\mathbf{x})\beta(\mathbf{x})\left(d_{xy}(\mathbf{x})\mathbf{a}_{xy}\mathbf{a}_{xy}^T + d\,\mathbf{a}_\perp\mathbf{a}_\perp^T\right) \\ &\quad + \kappa_2(\mathbf{x})d_z\mathbf{a}_z\mathbf{a}_z^T \\ &= \begin{bmatrix}\kappa_1(\mathbf{x})\cdot\mathbf{D}_{xy}(\mathbf{x}) & \mathbf{0} \\ \mathbf{0} & \kappa_2(\mathbf{x})\cdot d_z\end{bmatrix} \geq \mathbf{0}\end{aligned} \tag{28}$$

where d and d_z are positive damping constants of the undesirable directions $\mathbf{a}_\perp$ and $\mathbf{a}_z$ and the matrix $\mathbf{D}_{xy}(\mathbf{x})$ has the structure

$$\mathbf{D}_{xy}(\mathbf{x}) = \frac{\beta(\mathbf{x})}{1-q_p^2}\left(d_{xy}(\mathbf{x})\begin{bmatrix}q_x^2 & q_xq_y \\ q_xq_y & q_y^2\end{bmatrix} + d\begin{bmatrix}q_y^2 & -q_xq_y \\ -q_xq_y & q_x^2\end{bmatrix}\right). \tag{29}$$

The gains $1 \geq \kappa_1(\mathbf{x}) > 0$ and $1 \geq \kappa_2(\mathbf{x}) > 0$ in (28) serve to saturate the control torques. They are defined as

$$\kappa_1(\mathbf{x}) = \min_{\kappa>0,\,\|\mathbf{T}_{xy}-\kappa\,\mathbf{D}_{xy}\boldsymbol{\omega}_{xy}\|=\bar{\tau}_{xy}}(1,\kappa) \tag{30}$$

$$\kappa_2(\mathbf{x}) = \min_{\kappa>0,\,|\kappa\,d_z\omega_z|=\bar{\tau}_z}(1,\kappa) \tag{31}$$

where $\mathbf{T}_{xy} = [T_x\ \ T_y]^T$ and $\boldsymbol{\omega}_{xy} = [\omega_x\ \ \omega_y]^T$. The factor $\beta(\mathbf{x})$ in (29) is used to lower the x- and y-components of the damping torque down to zero if the error angle approaches $\varphi = \pi$ and thus accounts for the discontinuity of the decomposition (6). By choosing

$$\beta(\mathbf{x}) = \begin{cases}1 & \text{if} \quad 0 \leq \varphi \leq \varphi_u \\ \dfrac{\pi-\varphi}{\pi-\varphi_u} & \text{if} \quad \varphi_u < \varphi \leq \pi\end{cases} \tag{32}$$

we achieve that the total control torque $\boldsymbol{\tau} = \mathbf{T}(\mathbf{q}) - \mathbf{D}(\mathbf{x})\boldsymbol{\omega}$ is continuous at $\mathbf{q} = \begin{bmatrix}q_1 & q_2 & 0 & 0\end{bmatrix}$.

It remains to specify the function $d_{xy}(\mathbf{x})$ which is the damping about the axis $\mathbf{a}_{xy}$. To this end we start with some preliminary considerations. The moment of inertia matrix $\mathbf{J}$ of a quadrotor helicopter can usually be regarded as a diagonal matrix. Just for the specification of $d_{xy}(\mathbf{x})$ we take

$$\hat{\mathbf{J}} = \mathrm{diag}(\hat{J}_1, \hat{J}_1, \hat{J}_2) \tag{33}$$

as an estimate of $\mathbf{J}$. If (33) holds and if moreover $\boldsymbol{\omega} \parallel \mathbf{a}_{xy}$, then we have from (16), (20) (26) and (28) that $\dot{\boldsymbol{\omega}} \parallel \mathbf{a}_{xy}$. By multiplying Euler's equation (16) with $\mathbf{a}_{xy}^T$ from the left, allow for (22) and (23) and assume $\kappa_1(\mathbf{x}) = 1$ it finally reduces to the scalar differential equation

$$\hat{J}_1\ddot{\varphi} = \begin{cases}-c_\varphi\cdot\varphi - d_{xy}(\mathbf{x})\dot{\varphi} & \text{if} \quad 0 \leq \varphi \leq \varphi_l \\ \beta(\mathbf{x})(-c_\varphi\cdot\varphi_l - d_{xy}(\mathbf{x})\dot{\varphi}) & \text{if} \quad \varphi_l < \varphi\,.\end{cases} \tag{34}$$

This differential equation approximately holds in the unsaturated case ($\kappa_1(\mathbf{x}) = 1$) for a moment of inertia matrix similar to $\hat{\mathbf{J}}$ and angular velocities $\boldsymbol{\omega}$ with small components $\mathbf{a}_\perp^T\boldsymbol{\omega}$ and $\mathbf{a}_z^T\boldsymbol{\omega}$. The latter can be justified by the fact that these components of $\boldsymbol{\omega}$ are always damped. Assuming (34) holds, a damping strategy for different regions of the state space is developed in the following. Note that $\mathbf{J} = \hat{\mathbf{J}}$ is not required throughout this paper but good performance of the controller relies on $\mathbf{J}$ similar to $\hat{\mathbf{J}}$.

Around the desired thrust direction ($\varphi \le \varphi_l$) we wish to have linear dynamics in φ. Thus we choose

$$d_{xyI}(\mathbf{x}) = d \ge \sqrt{4\hat{J}_1 c_\varphi} \tag{35}$$

to be constant. Note that this choice yields aperiodic PT2 dynamics in (34) and according to (29) and (32) leads to a constant matrix $\mathbf{D}_{xy} = \mathrm{diag}(d, d)$. Thus $\mathbf{D}_{xy}$ is independent of $\mathbf{x}$ for $\varphi \le \varphi_l$ and the apparent singularity in (29) for $q_p = 1$ does not come into effect.

If the current thrust direction is far away from the desired one ($\varphi_l < \varphi$), a control strategy similar to time optimal control seems to be appropriate. This requires the computation of a switching curve $s(\varphi)$, where the control torque toggles from acceleration to deceleration. From (34) we notice that the potential energy causes a constant accelerating torque $-c_\varphi\,\varphi_l$ towards $\varphi = 0$ in the better part of the state space (as long as $\varphi \le \varphi_u$) and that we can add an arbitrary torque in the direction $-\dot{\varphi}$ by modifying the damping. Hence, in the acceleration phase we support $-c_\varphi\,\varphi_l$ best by adding damping if $\dot{\varphi} > 0$ and by keeping the damping zero if $\dot{\varphi} < 0$. In the deceleration phase we surely have $\dot{\varphi} < 0$ and thus can realize any braking torque by positive damping. The damping strategy given in the following additionally omits discontinuities in the control torque by interpolation. We choose

$$d_{xyII}(\mathbf{x}) = \begin{cases} d_{\mathrm{acc}}(\mathbf{x}) & \text{if} \quad \dot{\varphi} > r \cdot s(\varphi) \\ d_{\mathrm{mix}}(\mathbf{x}) & \text{if} \quad r \cdot s(\varphi) \ge \dot{\varphi} > s(\varphi) \\ d_{\mathrm{dec}}(\mathbf{x}) & \text{if} \quad s(\varphi) \ge \dot{\varphi} \end{cases} \tag{36}$$

where

$$d_{\mathrm{acc}}(\mathbf{x}) = \begin{cases} -\dfrac{c_\varphi\,\varphi_l}{\dot{\varphi}} + \dfrac{\tau_{\mathrm{br}}}{\dot{\varphi}} & \text{if} \quad \dot{\varphi} > \nu_1 \\ -\dfrac{c_\varphi\,\varphi_l}{\nu_1} + \dfrac{\tau_{\mathrm{br}}}{\nu_1} & \text{if} \quad \nu_1 \ge \dot{\varphi} > 0 \\ 0 & \text{if} \quad 0 \ge \dot{\varphi} \end{cases}, \tag{37}$$

$$d_{\mathrm{dec}}(\mathbf{x}) = -\frac{c_\varphi\,\varphi_l}{\dot{\varphi}} - \frac{\tau_{\mathrm{br}}}{\dot{\varphi}}, \tag{38}$$

$$d_{\mathrm{mix}}(\mathbf{x}) = d_{\mathrm{acc}}(\mathbf{x}) + \frac{\dot{\varphi} - r\,s(\varphi)}{(1-r)s(\varphi)}\left(d_{\mathrm{dec}}(\mathbf{x}) - d_{\mathrm{acc}}(\mathbf{x})\right), \tag{39}$$

$$s(\varphi) = -\sqrt{\nu_2^2 - 2\hat{J}_1^{-1}\tau_{\mathrm{br}}(\varphi_l - \varphi)} < 0, \tag{40}$$

and r, ν_1, ν_2, τ_{br} are positive constants. It is clear from (36) that the region of interpolation between acceleration and deceleration is determined by $0 < r < 1$. $\tau_{\mathrm{br}} \ge c_\varphi\varphi_l$ is the constant braking torque that is requested to slow down motion. This leads to an increasing damping for decreasing $\dot{\varphi}$. Thus the damping is held constant for $0 < \dot{\varphi} \le \nu_1$. The switching curve $s(\varphi)$ is chosen such that it describes the phase plane trajectory $\dot{\varphi}(\varphi)$ of the system $\hat{J}_1\ddot{\varphi} = \tau_{\mathrm{br}}$ which reaches $\varphi = \varphi_l$ with a velocity $\dot{\varphi} = -\nu_2$. Some considerations on the choice of the yet undetermined parameters are given in Sect. 6.

The overall damping $d_{xy}(\mathbf{x})$ is obtained by the interpolation between $d_{xyI}(\mathbf{x})$ and $d_{xyII}(\mathbf{x})$ according to

$$d_{xy}(\mathbf{x}) = \begin{cases} d_{xyI}(\mathbf{x}) & \text{if} \quad \varphi < \varphi_l \\ d_{xy\mathrm{mix}}(\mathbf{x}) & \text{if} \quad \varphi_l \le \varphi < \varphi_l + \Delta\varphi \\ d_{xyII}(\mathbf{x}) & \text{if} \quad \varphi_l + \Delta\varphi \le \varphi \end{cases} \tag{41}$$

with $d_{xy\mathrm{mix}}(\mathbf{x}) = d_{xyI}(\mathbf{x}) + \frac{\varphi - \varphi_l}{\Delta\varphi}(d_{xyII}(\mathbf{x}) - d_{xyI}(\mathbf{x}))$. The interpolation region is defined by the constant $\Delta\varphi$, which fulfills $\varphi_u - \varphi_l > \Delta\varphi > 0$.

5.4 Stability Properties

In the previous sections the control law (20) has been completely defined and we are now ready to state the stability result.

Theorem 1. *Application of the control law (20), with* $\mathbf{T}$ *defined by (26) and* $\mathbf{D}$ *defined by (28) to the plant dynamics (15) and (16), stabilizes the set of equilibrium points* $\mathcal{S} = \{\mathbf{x} \mid \mathbf{q} = [0\ \ 0\ \ q_3\ \ q_4]^T,\ \boldsymbol{\omega} = \mathbf{0}\}$ *almost globally asymptotically for arbitrary unknown moment of inertia matrices* $\mathbf{J}$ *and meets the constraints (17) regarding the bounded control torques.*

We first analyze the compliance with the constraints on the control inputs. According to (26) the induced torque has the structure $\mathbf{T} = [T_x\ \ T_y\ \ 0]^T = [\mathbf{T}_{xy}^T\ \ 0]^T$. Taking into account the definition of the damping matrix (28) the control law (20) can be written as

$$\boldsymbol{\tau} = \begin{bmatrix} \boldsymbol{\tau}_{xy} \\ \tau_z \end{bmatrix} = \begin{bmatrix} \mathbf{T}_{xy}(\mathbf{x}) - \kappa_1(\mathbf{x})\mathbf{D}_{xy}(\mathbf{x})\boldsymbol{\omega}_{xy} \\ 0 - \kappa_2(\mathbf{x})d_z\omega_z \end{bmatrix}. \tag{42}$$

Since $\|\mathbf{T}_{xy}\| = \|\mathbf{T}\| = T_\varphi$ and since we restricted the stiffness coefficient c_φ to lie in the interval $\bar{\tau}_{xy}/\varphi_l > c_\varphi > 0$, it is easily verified in (23) that $\|\mathbf{T}_{xy}\| < \bar{\tau}_{xy}$. It follows that there is always a positive $\kappa_1(\mathbf{x}) \le 1$ that solves the minimization problem (30), which guarantees $\|\boldsymbol{\tau}_{xy}\| = \sqrt{\tau_x^2 + \tau_y^2} \le \bar{\tau}_{xy}$. Analogously, a solution $1 \ge \kappa_2(\mathbf{x}) > 0$ of (31) always exists and ensures that $|\tau_z| \le \bar{\tau}_z$.

In the following we prove almost global asymptotic stability of the set $\mathcal{S}$ by applying La Salle's invariance principle, see e. g. [11]. Since $\dot{V}(\mathbf{x}) \le 0$, $\forall \mathbf{x} \in \mathcal{X}$ and since the level sets of $V(\mathbf{x})$ are compact, they are positively invariant and thus all solutions of the closed loop system starting in a certain level set must converge to an invariant set within that level set. Since $V(\mathbf{x})$ is bounded from below and $\dot{V}(\mathbf{x})$ is uniformly continuous (starting from (21) it can easily be verified that $\ddot{V}(\mathbf{x})$ is bounded), $\dot{V}(\mathbf{x}) \to 0$ as $t \to \infty$. Now let $\mathcal{E} = \{\mathbf{x} \mid \dot{V}(\mathbf{x}) = 0\}$, then all solutions of the closed loop system approach the largest

invariant set $\mathcal{M}$ in $\mathcal{E}$ as $t \to \infty$. The closed loop dynamics are given by

$$\dot{\mathbf{q}} = -\frac{1}{2}\mathbf{W}_R(\mathbf{q})\boldsymbol{\omega}\,, \tag{43}$$

$$\dot{\boldsymbol{\omega}} = \mathbf{J}^{-1}(\mathbf{J}\boldsymbol{\omega}\times\boldsymbol{\omega}) + \mathbf{J}^{-1}(\mathbf{T}(\mathbf{q}) - \mathbf{D}(\mathbf{x})\boldsymbol{\omega})\,. \tag{44}$$

Clearly, all equilibrium points are part of the set $\mathcal{M}$. By setting $\dot{\mathbf{x}} = \mathbf{0}$ in the closed loop system dynamics one obtains two sets of equilibrium points. The first is $\mathcal{S} = \{\mathbf{x} \,|\, \mathbf{q} = [0 \;\; 0 \;\; q_3 \;\; q_4]^T,\ \boldsymbol{\omega} = \mathbf{0}\}$ and the second is $\mathcal{U} = \{\mathbf{x} \,|\, \mathbf{q} = [q_1 \;\; q_2 \;\; 0 \;\; 0]^T,\ \boldsymbol{\omega} = \mathbf{0}\}$. By means of (21) one recognizes that the whole set $\mathcal{E}$ is given by the subset of $\mathcal{X}$ where $\mathbf{D}(\mathbf{x})\boldsymbol{\omega} = \mathbf{0}$. Apart from $\boldsymbol{\omega} = \mathbf{0}$, further solutions to $\mathbf{D}(\mathbf{x})\boldsymbol{\omega} = \mathbf{0}$ exist, since there is a set $\mathcal{Z}$ where the matrix $\mathbf{D}(\mathbf{x})$ has a rank defect caused by $d_{xy}(\mathbf{x}) = 0$ and $\beta(\mathbf{x}) = 0$ respectively. This can be verified using (28), (41), (36), (37) and (32). Accordingly, we have $\mathcal{E} = \mathcal{W} \cup \mathcal{Z}$ with

$$\mathcal{W} = \{\mathbf{x} \,|\, \boldsymbol{\omega} = \mathbf{0}\ ,\ \varphi \le \varphi_l + \Delta\varphi\}\,, \tag{45}$$

$$\begin{aligned}
&\mathcal{Z} = \mathcal{A} \cup \mathcal{B}\,,\\
&\mathcal{A} = \{\mathbf{x} \,|\, \boldsymbol{\omega} = k\cdot\mathbf{a}_{xy}\,,\ 0 \le k \le -r\cdot s(\varphi)\,,\\
&\qquad \varphi_l + \Delta\varphi \le \varphi < \pi\}\,,\\
&\mathcal{B} = \{\mathbf{x} \,|\, \boldsymbol{\omega} = k\cdot\mathbf{a}_{xy}\,,\ 0 \le k\,,\ \varphi = \pi\}
\end{aligned} \tag{46}$$

where $\mathcal{A}$ is the set where $d_{xy}(\mathbf{x}) = 0$ and $\mathcal{B}$ is the set where $\beta(\mathbf{x}) = 0$. Note that according to Remark 1 the vector $\mathbf{a}_{xy}$ in $\mathcal{B}$ can represent any direction in the whole xy-plane and thus stands for a two-dimensional space. Nevertheless we want to keep up the notation $\boldsymbol{\omega} = k\cdot\mathbf{a}_{xy}$ in $\mathcal{B}$ due to its connection with $\dot{\varphi}$ in (26).

Next we exclude the possibility of further invariant sets in $\mathcal{E}$, apart from the equilibrium sets $\mathcal{S}$ and $\mathcal{U}$. Let us start with the set $\mathcal{W}$, which contains $\mathcal{S}$. No further invariant sets can be contained in $\mathcal{W}$, since $\dot{\boldsymbol{\omega}} \neq \mathbf{0}$ everywhere in $\mathcal{W}\backslash\mathcal{S}$ and thus every trajectory starting there leaves $\mathcal{W}$ immediately. Next we notice that no trajectory leaving $\mathcal{W}$ can enter $\mathcal{Z}$. This is due to the fact that the angle φ in $\mathcal{W}$ is smaller (or equal) than in $\mathcal{Z}$. A trajectory leaving $\mathcal{W}$ and entering $\varphi > \varphi_l + \Delta\varphi$ necessarily needs a $\dot{\varphi} > 0$, which is not allowed in $\mathcal{Z}$. This can be seen by noting that for $\boldsymbol{\omega} = k\cdot\mathbf{a}_{xy}$ it holds that $k = -\dot{\varphi}$ and since $k \ge 0$ we have $\dot{\varphi} \le 0$, which corresponds to a decreasing or constant error angle. It remains to show that $\mathcal{Z}$ contains no invariant sets apart from $\mathcal{U}$. Note first that $\mathcal{U}$ is a subset of $\mathcal{B}$ and every trajectory starting in $\mathcal{B}\backslash\mathcal{U}$ leaves $\mathcal{B}$ immediately, since $k > 0$ implies $\dot{\varphi} < 0$. If $k \le -r\cdot s(\varphi)$, the trajectory enters $\mathcal{A}$. In the following we show that every trajectory with an initial state in $\mathcal{A}$ finally leaves $\mathcal{Z}$. Let us assume there is a complete trajectory starting in $\mathcal{A}$ and not leaving $\mathcal{Z}$. Then

$$\boldsymbol{\omega} = k\cdot\mathbf{a}_{xy} = -\dot{\varphi}\cdot\mathbf{a}_{xy} \tag{47}$$

for all times and the derivative is $\dot{\boldsymbol{\omega}} = \dot{k}\cdot\mathbf{a}_{xy} + k\cdot\dot{\mathbf{a}}_{xy}$. One can show that $\dot{\mathbf{a}}_{xy} = \mathbf{0}$ by using the definition of $\mathbf{a}_{xy}$ in (26), applying (10) and inserting the assumption (47). Hence, $\dot{\boldsymbol{\omega}}$ reduces to

$$\dot{\boldsymbol{\omega}} = \dot{k}\cdot\mathbf{a}_{xy}\,. \tag{48}$$

Remembering that in $\mathcal{A}$ the damping $d_{xy} = 0$ and $\boldsymbol{\omega}$ satisfies (47) we notice from (23), (26) and (28) that the control torque is given by $\boldsymbol{\tau} = T_\varphi(\varphi)\cdot\mathbf{a}_{xy}$. Thus the derivative of the rotational energy is

$$\dot{E}_{rot} = \boldsymbol{\omega}^T\boldsymbol{\tau} = k\cdot\mathbf{a}_{xy}^T\cdot T_\varphi(\varphi)\cdot\mathbf{a}_{xy} = k\cdot T_\varphi(\varphi)\,. \tag{49}$$

On the other hand we obtain

$$\dot{E}_{rot} = \boldsymbol{\omega}^T\mathbf{J}\dot{\boldsymbol{\omega}} = k\dot{k}\cdot\mathbf{a}_{xy}^T\mathbf{J}\mathbf{a}_{xy} \tag{50}$$

by using (47) and (48). Inserting (49) in (50) and solving for $-\dot{k} = \ddot{\varphi}$ gives

$$\ddot{\varphi} = -\frac{T_\varphi(\varphi)}{\mathbf{a}_{xy}^T\mathbf{J}\mathbf{a}_{xy}} = \begin{cases} -\dfrac{c_\varphi\varphi_l}{\mathbf{a}_{xy}^T\mathbf{J}\mathbf{a}_{xy}} & \text{if} \quad \varphi \le \varphi_u \\ -\dfrac{c_\varphi\varphi_l\cdot(\pi-\varphi)}{\mathbf{a}_{xy}^T\mathbf{J}\mathbf{a}_{xy}(\pi-\varphi_u)} & \text{if} \quad \varphi_u < \varphi\,. \end{cases} \tag{51}$$

The solutions of these two linear differential equations are

$$\varphi(t) = \begin{cases} -\dfrac{1}{2}\dfrac{c_\varphi\varphi_l}{\mathbf{a}_{xy}^T\mathbf{J}\mathbf{a}_{xy}}\cdot t^2 + \dot{\varphi}_0\cdot t + \varphi_0\,, & \text{if} \quad \varphi \le \varphi_u \\ A\cdot e^{\sqrt{b}t} + B\cdot e^{-\sqrt{b}t} + \pi\,, & \text{if} \quad \varphi_u < \varphi \end{cases} \tag{52}$$

where $b = \frac{c_\varphi\varphi_l}{\mathbf{a}_{xy}^T\mathbf{J}\mathbf{a}_{xy}(\pi-\varphi_u)} > 0$, $A = \left(\frac{\varphi_0-\pi}{2} + \frac{\dot{\varphi}_0}{2\sqrt{b}}\right)$ and $B = \left(\frac{\varphi_0-\pi}{2} - \frac{\dot{\varphi}_0}{2\sqrt{b}}\right)$. Let us first assume an initial state $\mathbf{x}_0 \in \mathcal{A}$ with a corresponding $\varphi_0 > \varphi_u$ and $\dot{\varphi}_0 \le 0$. As long as $\varphi(t) > \varphi_u$ the second solution in (52) is valid. Note that for the assumed initial state $A < 0$ and thus $\varphi(t)$ leaves $\varphi > \varphi_u$ and enters $\varphi \le \varphi_u$. From there on the first solution in (52) is valid. For any initial state $\mathbf{x}_0 \in \mathcal{A}$ with a corresponding $\varphi_0 \le \varphi_u$ and $\dot{\varphi}_0 \le 0$ the first solution in (52) shows that the error angle $\varphi(t)$ decreases until it falls below $\varphi_l + \Delta\varphi$ and thus leaves $\mathcal{Z}$. Note that $\mathcal{Z}$ might also be left because $\dot{\varphi}$ falls below $r\cdot s(\varphi)$. We conclude that apart from $\mathcal{U}$ no invariant sets are contained in $\mathcal{Z}$. It follows that all solutions of the closed loop system either approach $\mathcal{S}$ or $\mathcal{U}$. If we choose any initial state $\mathbf{x}_0$, such that $V(\mathbf{x}_0) < E_{pot}(\pi)$, we exclude $\mathcal{U}$ from the initial level set of $V(\mathbf{x})$ and the solution can only approach $\mathcal{S}$. Hence, $\mathcal{S}$ is an asymptotically stable set of equilibrium points. The preceding argumentation also proves that $\mathcal{U}$ contains only unstable equilibrium points, and therefore can only be attractive to the trajectories in an invariant manifold of smaller dimension than the state space. It is known that an m-dimensional invariant manifold of an n-dimensional system has Lebesgue measure zero if $m < n$, see [14]. Consequently, the set of initial conditions that converges to $\mathcal{U}$ has zero measure. The preceding argumentation does not require any knowledge of the moment of inertia matrix $\mathbf{J}$ in the control law. □

6 Simulation Results

In this section we present simulation results for two different initial conditions illustrating the performance of the controller. The plant and controller parameters together with the initial states of the first and the second regulation process are given in Table 1. For each initial condition the same controller was tested with 51 plants differing by their moment of inertia matrix. We will call the plant with the diagonal moment of inertia matrix $\mathbf{J} = \hat{\mathbf{J}}$ the nominal plant and all lines in Figs. 3 and 4 show the results for the corresponding nominal closed loop system. The remaining 50 moment of inertia matrices are given by $\mathbf{J} = \hat{\mathbf{J}} + \Delta\mathbf{J}$ where $\Delta\mathbf{J}$ represents different uncertainty matrices, which were chosen as symmetric normally distributed random matrices with all elements constrained by $-0.1 \cdot (\hat{\mathbf{J}})_{11} \leq (\Delta\mathbf{J})_{ij} \leq 0.1 \cdot (\hat{\mathbf{J}})_{11}$. The shaded areas in Figs. 3 and 4 span the regions which contain the simulation results for those 50 cases. For reasons of clarity and readability no shaded areas are given for τ_x and τ_y.

The following considerations have been the basis for the controller parametrization. The stiffness coefficient c_φ was chosen such that $c_\varphi = 0.95 \cdot \bar{\tau}_{xy}/\varphi_l$ holds. While on the one hand it is desirable to have c_φ as large as possible, it was illustrated in Sect. 5.3 that the angular velocity component $\mathbf{a}_\perp^T \boldsymbol{\omega}$ should always be damped. This can only be guaranteed if T_φ is always smaller than $\bar{\tau}_{xy}$ or accordingly $c_\varphi < \bar{\tau}_{xy}/\varphi_l$. The chosen c_φ ensures that $\mathbf{a}_\perp^T \boldsymbol{\omega}$ can always be damped with at least $\sqrt{0.05} \cdot \bar{\tau}_{xy} \approx 0.22 \cdot \bar{\tau}_{xy}$. The maximum torque $\bar{\tau}_{xy}$ was chosen as the braking torque τ_{br} that is requested by the "time optimal" strategy to slow down the motion of φ in the region $\varphi > \varphi_l + \Delta\varphi$. This enables the controller to decelerate as late as possible. The damping coefficient d was chosen to be 1.2 times the critical damping $\sqrt{4\hat{J}_1 c_\varphi}$ of the PT2-dynamics in (34) resulting in a well damped aperiodic behavior for $\varphi \leq \varphi_l$. Finally the angular velocity constant v_2 characterizing the negative entrance angular velocity $-\dot{\varphi}$ at $\varphi = \varphi_l$ when moving along the switching curve $s(\varphi)$, was chosen such that $-c_\varphi \cdot \varphi_l + d \cdot v_2 = 0.95 \cdot \bar{\tau}_{xy}$ holds.

The initial conditions 1 and 2 describe a situation where the quadrotor helicopter needs to rotate $170 \cdot \pi/180$ rad around its x-axis to align the thrust with the

Table 1 Controller parameters, plant parameters and initial conditions of the simulations.

Controller parameters	Plant parameters
$\varphi_l = 10 \times \frac{\pi}{180}$ rad	$\hat{\mathbf{J}} = \mathrm{diag}(8.5, 8.5, 14) \times 10^{-3}\ \mathrm{m^2\,kg}$
$\varphi_u = 175 \times \frac{\pi}{180}$ rad	$\mathbf{J} = \hat{\mathbf{J}} + \Delta\mathbf{J}\ \mathrm{m^2\,kg}$
$\Delta\varphi = 5 \times \frac{\pi}{180}$ rad	$\bar{\tau}_{xy} = 0.15$ Nm
$c_\varphi = 0.817 \frac{\mathrm{Nm}}{\mathrm{rad}}$	$\bar{\tau}_z = 0.03$ Nm
$d = 0.1999 \frac{\mathrm{Nms}}{\mathrm{rad}}$	**Initial condition 1**
$d_z = 0.1666 \frac{\mathrm{Nms}}{\mathrm{rad}}$	$\varphi_0 = 170 \times \frac{\pi}{180}$ rad
$\tau_{\mathrm{br}} = 0.15$ Nm	$\mathbf{q}_0 = \left[\sin\left(\frac{\varphi_0}{2}\right)\ 0\ 0\ \cos\left(\frac{\varphi_0}{2}\right)\right]^T$
$v_1 = 0.1 \frac{\mathrm{rad}}{\mathrm{s}}$	$\boldsymbol{\omega}_0 = [-2.5\ 0\ 0]^T \frac{\mathrm{rad}}{\mathrm{s}}$
$v_2 = 1.425 \frac{\mathrm{rad}}{\mathrm{s}}$	**Initial condition 2**
$r = 0.75$	$\varphi_0 = 170 \times \frac{\pi}{180}$ rad
	$\mathbf{q}_0 = \left[\sin\left(\frac{\varphi_0}{2}\right)\ 0\ 0\ \cos\left(\frac{\varphi_0}{2}\right)\right]^T$
	$\boldsymbol{\omega}_0 = [0\ 0\ 1.7]^T \frac{\mathrm{rad}}{\mathrm{s}}$

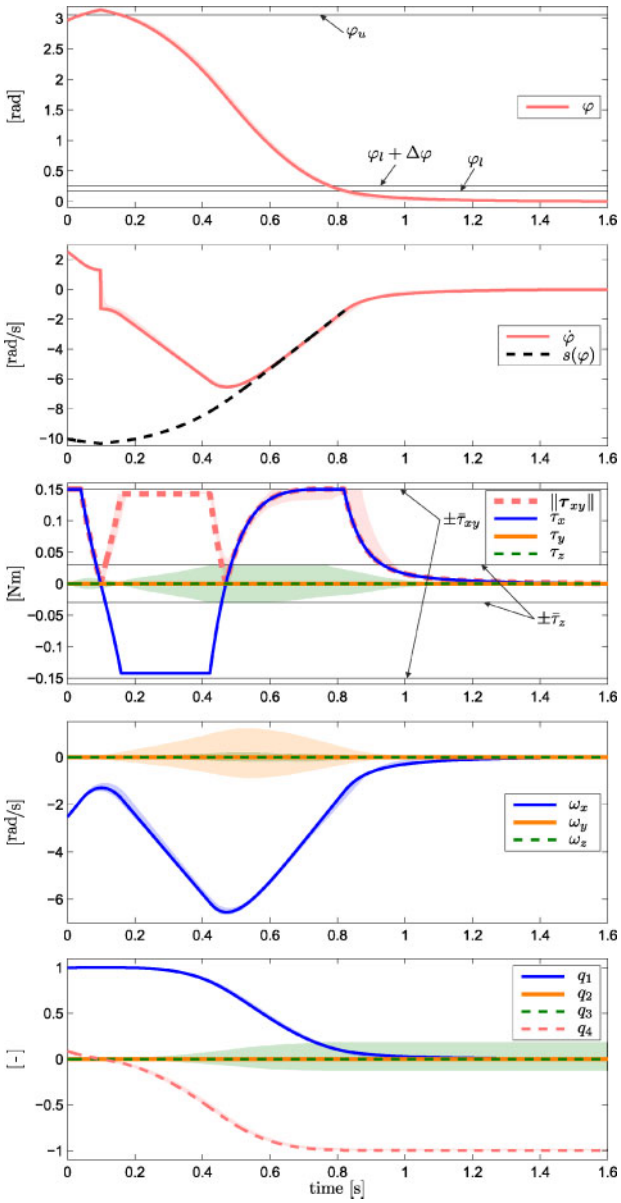

Figure 3 Simulation results for initial condition 1. Lines: Nominal closed loop. Shaded Areas: Closed loops with $\mathbf{J} = \hat{\mathbf{J}} + \Delta\mathbf{J}$.

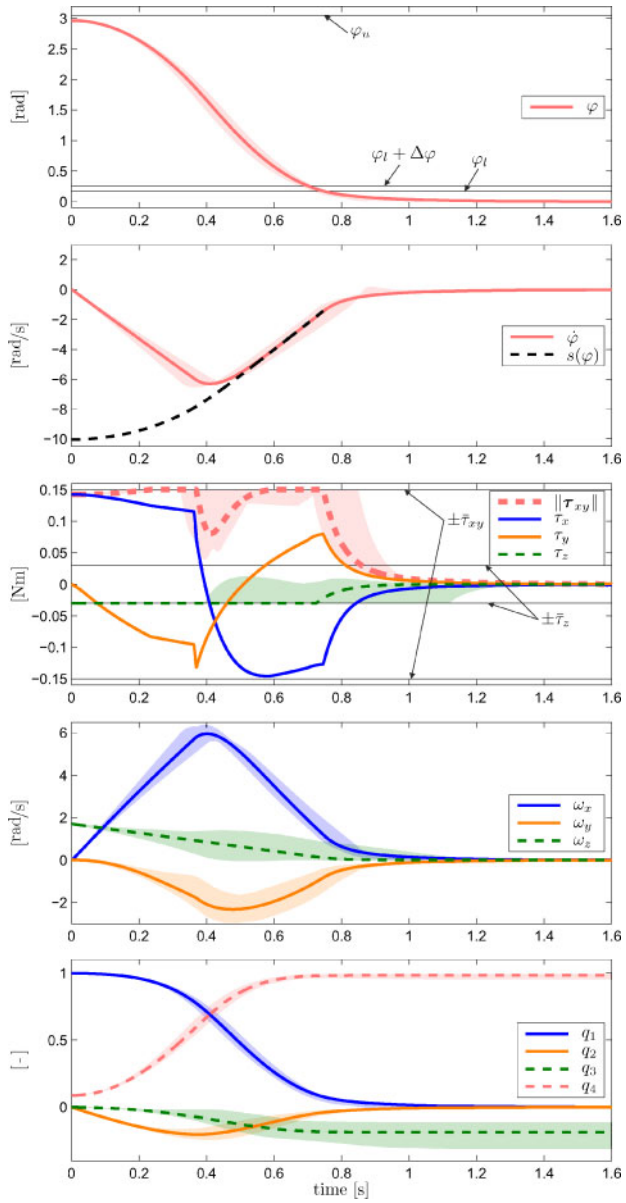

Figure 4 Simulation results for initial condition 2. Lines: Nominal closed loop. Shaded Areas: Closed loops with $\mathbf{J} = \hat{\mathbf{J}} + \Delta\mathbf{J}$.

desired thrust direction. In the first case, shown in Fig. 3 the quadrotor helicopter has a initial angular velocity that rotates the current thrust directly away from its target direction. The control torque acts against this motion, but cannot completely stop it before φ reaches π meaning that the thrust points into the opposite direction of the desired one. The quadrotor helicopter then flips over and now a negative rotation about its x-axis is the shortest way to the desired thrust direction. Hence the control torque now accelerates the motion until $\dot{\varphi}$ has approached the switching curve $s(\varphi)$ and the behavior changes from acceleration to deceleration. The current thrust direction finally enters $\varphi \leq \varphi_l$, from where on a soft transient to the equilibrium point follows. Note that since in the nominal case $\mathbf{J}$ fulfills (33) and ω_{y0} and ω_{z0} are zero, we have the special case that (34) is exactly satisfied for all times. It can be seen by the shaded areas that for the nonnominal plants ω_y and ω_z can go away from zero and that different equilibrium points in the set $\mathcal{S}$ are approached. Note also that in all cases the control torques are compliant with the input constraints and that moreover the available control torques are very well exploited during the regulation process. The control inputs are even saturating over a significant amount of time. For all plants the desired thrust direction is reached after approximately 1.2 s.

The angular velocity $\boldsymbol{\omega}_0$ of the initial condition 2 has a nonzero component ω_z that has to be slowed down during the regulation process. It can be seen in Fig. 4 that the full available torque $\bar{\tau}_z$ is used to do that. The appearance of a nonzero ω_z has different effects. On the one hand it causes the axis vector $\mathbf{a}_{xy}$, which describes the desired rotation axis in the B frame, to circulate in the xy-plane and accordingly the direction of $\mathbf{T}$ moves along. On the other hand it causes nonzero $\mathbf{a}_{\perp}^{T}\boldsymbol{\omega}$ components even for the nominal system via the Coriolis-term in (16). As a result all components of $\boldsymbol{\tau}$ are needed during the regulation process. Note that also in this case we have a very good exploitation and in wide areas even saturation of the available control torques. The settling time is again approximately 1.2 s.

7 Conclusion

In this paper, we have presented a fast and saturating thrust direction controller for a quadrotor helicopter. The nonlinear controller is based on an energy shaping approach and considers the full nonlinear nature of the plant including control input constraints. Almost global asymptotic stability of the desired thrust direction has been shown for arbitrary unknown moment of inertia matrices. The performance of the controller has been illustrated by simulations, which also have shown that the available control torques are exploited to a great extent or even saturated. The very short settling time of the closed loop system is facilitated by the fact that thrust direction control does not require to specify the orientation of the quadrotor helicopter around its thrust axis. Nevertheless the augmentation of the presented controller to a complete attitude controller is possible and is the current work of the authors. The intention is to design an attitude controller which still prioritizes the alignment of the thrust and leads to a more or less sequential completion of the attitude control task. It will be interesting to analyze the robustness of the proposed controller in the presence of influences like actuator, sensor and observer dynamics as well as gyroscopic and aerodynamic effects. First experiments with the presented controller are currently in progress and will reveal its properties.

References

[1] I. Ali and G. Radice. Autonomous attitude control using potential function method under control input saturation. In *Proceedings of the 59th International Astronautical Congress*, 2008.

[2] S. P. Bhat and D. S. Bernstein. A topological obstruction to continuous global stabilization of rotational motion and the unwinding phenomenon. *Systems & Control Letters*, 39(1):63–70, Jan. 2000.
[3] M. Bouchoucha, S. Seghour, and M. Tadjine. Classical and second order sliding mode control solution to an attitude stabilization of a four rotors helicopter: From theory to experiment. In *Proceedings of the IEEE International Conference on Mechatronics (ICM)*, pages 162–169, Apr. 2011.
[4] M. Buhl, O. Fritsch, and B. Lohmann. Exakte Ein-/Ausgangslinearisierung für die translatorische Dynamik eines Quadrocopters. *at – Automatisierungstechnik*, 59(6):374–381, 2011.
[5] N. A. Chaturvedi, N. H. McClamroch, and D. S. Bernstein. Asymptotic smooth stabilization of the inverted 3D pendulum. *IEEE Transactions on Automatic Control*, 54:1204–1215, June 2009.
[6] M. Dalsmo and O. Egeland. State feedback H_∞-suboptimal control of a rigid spacecraft. *IEEE Transactions on Automatic Control*, 42(8):1186–1191, 1997.
[7] O. Fritsch, P. De Monte, M. Buhl, and B. Lohmann. Quasi-static feedback linearization for the translational dynamics of a quadrotor helicopter. In *Proceedings of the American Control Conference*, 2012.
[8] J. F. Guerrero-Castellanos, N. Marchand, S. Lesecq, and J. Delamare. Bounded attitude stabilization: Real-time application on four-rotor mini-helicopter. In *Proceedings of the 17th IFAC World Congress*, 2008.
[9] M.-D. Hua, T. Hamel, P. Morin, and C. Samson. A control approach for thrust-propelled underactuated vehicles and its application to VTOL drones. *IEEE Transactions on Automatic Control*, 54(8):1837–1853, Aug. 2009.
[10] S. M. Joshi, A. G. Kelkar, and J. T.-Y. Wen. Robust attitude stabilization of spacecraft using nonlinear quaternion feedback. *IEEE Transactions on Automatic Control*, 40(10):1800–1803, 1995.
[11] H. K. Khalil. *Nonlinear systems*. Prentice Hall, Upper Saddle River, NJ, 1996.
[12] N. Kottenstette and J. Porter. Digital passive attitude and altitude control schemes for quadrotor aircraft. In *IEEE International Conference on Control and Automation (ICCA)*, pages 1761–1768, Dec. 2009.
[13] M. Krstic and P. Tsiotras. Inverse optimal stabilization of a rigid spacecraft. *IEEE Transactions on Automatic Control*, 44(5):1042 – 1049, May 1999.
[14] M. Krstic, J. W. Modestino, and H. Deng. *Stabilization of Nonlinear Uncertain Systems*. Springer-Verlag New York, Inc., 1998.
[15] T. Lee. Geometric tracking control of the attitude dynamics of a rigid body on SO(3). In *Proceedings of the American Control Conference*, pages 1200–1205, 2011.
[16] C. G. Mayhew, R. G. Sanfelice, and A. R. Teel. Quaternion-based hybrid control for robust global attitude tracking. *IEEE Transactions on Automatic Control*, 56:2555–2566, Nov. 2011.
[17] R. Ortega, A. J. Van Der Schaft, I. Mareels, and B. Maschke. Putting energy back in control. *IEEE Control Systems Magazine*, 21(2):18–33, 2001.
[18] K. Rudin, M.-D. Hua, G. Ducard, and S. Bouabdallah. A robust attitude controller and its application to quadrotor helicopters. In *Proceedings of the 18th IFAC World Congress*, pages 10379–10384, 2011.
[19] M. Shuster. A survey of attitude representations. *The Journal of the Astronautical Sciences*, 41(4):439–517, 1993.
[20] A. Tayebi. Unit quaternion-based output feedback for the attitude tracking problem. *IEEE Transactions on Automatic Control*, 53(6):1516–1520, 2008.
[21] A. Tayebi and S. McGilvray. Attitude stabilization of a VTOL quadrotor aircraft. *IEEE Transactions on Control Systems Technology*, 14(3):562–571, May 2006.
[22] J. T. Y. Wen and K. Kreutz-Delgado. The attitude control problem. *IEEE Transactions on Automatic Control*, 36(10):1148–1162, Oct. 1991.
[23] J. Wertz. *Spacecraft Attitude Determination and Control*. Kluwer Academic Publishers, Boston, 2002.

Received: May 16, 2012

Dipl.-Ing. Oliver Fritsch arbeitet am Lehrstuhl für Regelungstechnik im Bereich nichtlineare Regelungen. Hauptarbeitsgebiete: Nichtlineare Regelungsstrategien für Quadrocopter.

Address: Lehrstuhl für Regelungstechnik, Technische Universität München, Fakultät Maschinenwesen, Boltzmannstr. 15, D-85748 Garching bei München, Fax: +49-(0)89-289-15653,
e-mail: oliver.fritsch@tum.de

Dipl.-Ing. Bernd Henze hat an der TU München Mechatronik und Infomationstechnik studiert und seine Diplomarbeit am Lehrstuhl für Regelungstechnik verfasst.

Address: e-mail: bernd.henze@mytum.de

Prof. Dr.-Ing. habil. Boris Lohmann ist Leiter des Lehrstuhls für Regelungstechnik der Fakultät Maschinenwesen der TU München. Hauptarbeitsgebiete: Modellreduktion, nichtlineare, robuste und optimale Regelung, aktive Schwingungsdämpfung, industrielle Anwendungen.

Address: Lehrstuhl für Regelungstechnik, Technische Universität München, Fakultät Maschinenwesen, Boltzmannstr. 15, D-85748 Garching bei München, Fax: +49-(0)89-289-15653,
e-mail: lohmann@tum.de

An der Technischen Universität Graz/
Fakultät für Elektrotechnik und
Informationstechnik ist die Professur

TU Graz
Graz University of Technology

Regelungs- und Automatisierungstechnik

mit dem Schwerpunkt Regelungstechnik am Institut für Regelungs- und Automatisierungstechnik (Nachfolge O.Univ.-Prof. Dr.-Ing. Dourdoumas) ab 1.10.2013 zu besetzen. Der/die Universitätsprofessor/in wird in einem unbefristeten Arbeitsverhältnis angestellt und in die Verwendungsgruppe A1 des Kollektivvertrages für die ArbeitnehmerInnen der Universitäten eingereiht. Eine Überzahlung des kollektivvertraglichen monatlichen Mindestgehaltes von € 4.571,20 (14x jährlich) kann vereinbart werden.

Gesucht wird eine hervorragend qualifizierte und wissenschaftlich ausgewiesene Persönlichkeit, die das Fachgebiet Regelungstechnik in Forschung und Lehre mit Engagement vertreten kann. Von den Bewerberinnen und Bewerbern wird erwartet, dass sie ein anspruchsvolles, methoden- und anwendungsorientiertes Forschungsprogramm im Bereich der Regelungstechnik bearbeiten.

Die Technische Universität Graz strebt eine Erhöhung des Frauenanteiles, insbesondere in Leitungsfunktionen und beim wissenschaftlichen Personal, an und lädt deshalb qualifizierte Frauen ausdrücklich zur Bewerbung ein. Bei gleicher Qualifikation werden Frauen vorrangig aufgenommen.

Die Bewerbungsunterlagen sind in schriftlicher und elektronischer Form bis spätestens **2. April 2013** (Datum des Poststempels/E-Mail-Eingangs, an den Dekan der Fakultät für Elektrotechnik und Informationstechnik der Technischen Universität Graz, Herrn Univ.-Prof. Dipl.-Ing. Mag. Dr. Heinrich Stigler, Inffeldgasse 18/EG, A-8010 Graz, E-Mail: **dekanat.etit@tugraz.at** zu übermitteln.

Weitere Informationen sowie die Anstellungserfordernisse entnehmen Sie bitte der Homepage

www.e-i.tugraz.at/dekanat

Der Dekan: Stigler